

Storm/Quiet Ratio Comparisons Between TIMED/SABER $\text{NO}^+(\nu)$ Volume Emission Rates and Incoherent Scatter Radar Electron Densities at E-Region Altitudes

J.R. Fernandez¹, C. J. Mertens¹, D. Bilitza², X. Xu³, J. M. Russell III⁴, and M. G. Mlynczak¹

¹NASA Langley Research Center, Hampton, VA USA

²George Mason University, Fairfax, VA USA

³SSAI, Inc., Hampton, VA USA

⁴Hampton University, Hampton, VA USA

Abstract

Broadband infrared limb emission at 4.3 μm is measured by the TIMED/SABER instrument. At night, these emission observations at E-region altitudes are used to derive the so called $\text{NO}^+(\nu)$ Volume Emission Rate (VER). $\text{NO}^+(\nu)$ VER can be derived by removing the background $\text{CO}_2(\nu_3)$ 4.3 μm radiance contribution using SABER-based non-LTE radiation transfer models, and by performing a standard Abel inversion on the residual radiance. SABER observations show that $\text{NO}^+(\nu)$ VER is significantly enhanced during magnetic storms in accordance with increased ionization of the neutral atmosphere by auroral electron precipitation, followed by vibrational excitation of NO^+ (i.e., $\text{NO}^+(\nu)$) from fast exothermic ion-neutral reactions, and prompt infrared emission at 4.3 μm . Due to charge neutrality, the $\text{NO}^+(\nu)$ VER enhancements are highly correlated with electron density enhancements, as observed for example by Incoherent Scatter Radar (ISR). In order to characterize the response of the storm-time E-region from both SABER and ISR measurements, a Storm/Quiet ratio (SQR) quantity is defined as a function of altitude. For SABER, the SQR is the ratio of the storm-to-quiet $\text{NO}^+(\nu)$ VER. SQR is the storm-to-quiet ratio of electron densities for ISR. In this work, we compare SABER and ISR SQR values between 100 to 120 km. Results indicate good agreement between these measurements. SQR values are intended to be used as a correction factor to be included in an empirical storm-time correction to the International Reference Ionosphere model at E-region altitudes.

Keywords: Infrared remote sensing; Ionosphere; E-region; Magnetic storm; SABER

1. Introduction

The Sounding of the Atmosphere using Broadband Emission Radiometry (SABER) instrument is a multi-channel radiometer onboard the Thermosphere-Ionosphere-Mesosphere-Energetics and Dynamics (TIMED) satellite. TIMED was successfully launched in December, 2001. Continuous SABER measurements began in January 2002. SABER scans the Earth's limb line-of-sight and radiance measurements are made by 10 broadband radiometer channels from 1.27 μm to 17 μm . Depending on the specific data

product, geophysical parameters are derived at tangent altitudes ranging from the tropopause to over 180 km. Daytime and nighttime measurements are made over a latitude range that alternates hemispheres in a 60-day yaw period, extending to 83 degrees in one hemisphere to 52 degrees in the opposite hemisphere. After approximately 60 days the TIMED satellite performs a yaw maneuver and hemispheric coverage is reversed, as depicted in Fig. 1. Dashed lines in Fig. 1 indicate dates of the yaw maneuvers for the year 2003. Similar yaw dates are performed every year. Additional information about SABER instrument can be found in Russell et al. (1999).

We observed that radiance measurements at 4.3 μm were significantly increased during geomagnetic disturbances, such as during the Halloween 2003 superstorm events reported by Mertens et al. (2007a). These enhancements are due to vibrationally excited NO^+ emissions produced by precipitating auroral electrons, which ionize the neutral atmosphere. At E-region altitudes, these ions react with neutral species to produce NO^+ (Torr et al., 1990; Fox and Sung, 2001). Moreover, some of these reactions are exothermic enough to produce $\text{NO}^+(\text{v})$ emissions at 4.3 μm . In order to isolate the $\text{NO}^+(\text{v})$ emissions, a new $\text{NO}^+(\text{v})$ Volume Emission Rate (VER) data product was produced by eliminating the $\text{CO}_2(\text{v}_3)$ contribution from the measured radiances using non-local thermodynamic equilibrium (non-LTE) algorithms, and performing a standard Abel inversion on the residuals. This procedure is applied to nighttime 4.3 μm measurements since $\text{CO}_2(\text{v}_3)$ contributions are dominant during daytime. Figure 2 shows an example of both radiance and VER measurements for two measurement scans: before (blue line) and during (red line) the Halloween 2003 magnetic storm. Note that at quiet times, radiances values reach the 4.3 μm channel detector noise limit, denoted by the Noise Equivalent Radiance (NER), at about 135 km. During the magnetically disturbed periods, the 4.3 μm limb radiance measurements do not reach the noise limit until above 180 km. Storm-enhanced radiances are increased by several orders of magnitude compared to quiescent values. VER values are also enhanced as shown in the right panel.

VER enhancements can be used as a proxy to characterize electron density during magnetic storm periods by comparing them to quiet time profiles (Mertens, et al., 2007b). This characterization led to the idea of using storm-to-quiet time ratios (SQR) to generate a correction factor for the International Reference Ionosphere (IRI) model. The IRI model is an empirical model widely used in the ionospheric community to obtain climatological mean values for the electron density, electron and ion temperatures, among other parameters (Bilitza, 2001). However, uncertainties still remain as to how ionosphere parameters are affected under magnetic storm conditions, especially at E-region altitudes. In this work, we validate our so-called SQR quantity by comparing Incoherent Scatter Radar (ISR) with SABER $\text{NO}^+(\text{v})$ VER measurements for particular magnetic storm events.

In a future work, the SABER $\text{NO}^+(\text{v})$ VER SQR will form the basis for an empirical correction to E-region electron densities during geomagnetic disturbances, and applied to the IRI, as briefly described section 2. In order to develop the empirical correction, we will derive a parametric relation between SABER $\text{NO}^+(\text{v})$ VER SQR and an appropriate magnetic index. In order to select an appropriate index, we derive the cross-correlation

function between SABER $\text{NO}^+(\text{v})$ VER and the most common and widely used geomagnetic indices. The cross-correlation functions are computed for the Halloween 2003 storm period, which are presented in section 3. In section 4 we show SQR comparisons between ISR and SABER $\text{NO}^+(\text{v})$ VER for different storm events and ISR locations. Our conclusions are given in section 5.

2. Storm-time correction model

SABER $\text{NO}^+(\text{v})$ VER measurements provide a new useful tool for monitoring the ionosphere at nighttime during magnetic storm-time periods. By computing storm-to-quiet ratios, they can be used as a proxy to estimate the electron density enhancements at E-region altitudes. Thus, SQR values denoted by r are defined by

$$r(z, \lambda_m, \varphi_m, t) = \frac{\text{VER}_{\text{Storm}}(z, \lambda_m, \varphi_m, t)}{\text{VER}_{\text{Quiet}}(z, \lambda_m, \varphi_m)}, \quad (1)$$

where z , t , λ_m , and φ_m are altitude, UT-time, magnetic latitude, and magnetic longitude (or magnetic local time), respectively. Quiet $\text{NO}^+(\text{v})$ VER observations are time independent, by definition, since they represent a climatological average over a period of magnetic quiet time. Since the SABER VER in (1) are due to $\text{NO}^+(\text{v})$ emissions, and since NO^+ is the terminal E-region ion, the SQR values can be approximated by

$$r(z, \lambda_m, \varphi_m, t) \approx \frac{[\text{NO}^+]_{\text{Storm}}}{[\text{NO}^+]_{\text{Quiet}}} \approx \frac{[e]_{\text{Storm}}}{[e]_{\text{Quiet}}} \quad (2)$$

where $[e]$ is the electron density at storm or quiet times, respectively. Equations (1)-(2) represent the fundamental basis of our storm-time E-region electron density correction, and (2) is the relation we seek to validate in this work. The $[\text{NO}^+]$ SQR can be estimated by SABER $\text{NO}^+(\text{v})$ VER observations and the $[e]$ SQR can be calculated using ISR data, as described later in section 4. Once this ratio is computed, it can be used as a storm-time E-region electron density correction factor for the IRI model, i.e.,

$$[NmE(t)]_{\text{Storm}}^{\text{IRI}}(\text{peak}) = \tilde{r}(\lambda_m, \varphi_m, t) \times [NmE]_{\text{Nominal}}^{\text{IRI}}(\text{peak}). \quad (3)$$

Thus, the SABER-derived $\text{NO}^+(\text{v})$ VER SQR values can scale the nominal quiescent IRI E-region electron density peak, $[NmE]_{\text{Nominal}}^{\text{IRI}}(\text{peak})$, to obtain a storm-enhanced E-region electron density peak value. The SQR in (3) is given by an average over altitude:

$$\tilde{r}(\lambda_m, \varphi_m, t) = \frac{1}{\Delta z} \int_{Z_B}^{Z_T} r(z, \lambda_m, \varphi_m, t) dz. \quad (4)$$

The terms $Z_{B,T}$ represent the bottom and top altitude limits of integration, respectively, and Δz is the altitude interval. The top and bottom altitude limits in (4) are determined from our SABER/ISR SQR validation studies. Our validations studies presented in

section 4 suggest that the bottom and top altitude limits of integration should be 115 km and 120 km, respectively. The physical rationale for these altitude integration limits will be discussed in detail in a future report.

The SQR defined in (1) can also be expanded in terms of a magnetic forcing parameter (G):

$$r(z, \lambda_m, \varphi_m; t) = \sum_{i=0}^N a_i(z, \lambda_m, \varphi_m) G^i(z, \lambda_m, \varphi_m; t), \quad (5)$$

where a_i are the expansion coefficients. The magnetic forcing parameter represents the E-region response to a magnetic storm event. Therefore, it can be expressed as a convolution between an impulse response function F and a magnetic index D such as

$$G(z, \lambda_m, \varphi_m; t) = \int_{-T_s}^T F(z, \lambda_m, \varphi_m; \tau) D(t - \tau) d\tau. \quad (6)$$

The upper limit of the integral above is referred to as the effective memory of the storm-time response of the E-region (T) and the lower limit is the start time of the event (T_s). Magnetic index parameters such as the Hemispheric Power index (HP), Disturbed Storm Time (Dst), ap index, and the Auroral Electroject (AE) index, can be considered as possible candidates for the magnetic index D . Finally, from Equations (5) and (6), and assuming a linear impulse-response relation between the external driver index and the SABER NO⁺(v) VER SQR data, the response function can be determined by

$$r(z, \lambda_m, \varphi_m; t) = \int_{-T_s}^T F(z, \lambda_m, \varphi_m; \tau) D(t - \tau) d\tau. \quad (7)$$

The above equation can be discretized and solved by matrix inversion using standard Singular Value Decomposition (SVD) techniques (Press et al., 1992). In the next section, a cross-correlation approach to determine the magnetic index described in (6) and (7) is presented.

3. Halloween 2003 cross-correlation analysis

In this section, SABER NO⁺(v) VER data from the Halloween 2003 magnetic storm period is cross-correlated with commonly used magnetic indices to determine which magnetic driver index should be used in (6). The cross-correlation function is defined as (Vassiliadis, 2002)

$$C(\lambda_m, \tau) = \frac{1}{T} \frac{1}{\sigma_D \sigma_{\text{VER}}} \sum_{i=1}^T (\text{VER}(\lambda_m, t_i + \tau) - \langle \text{VER}(\lambda_m) \rangle) (D(t_i) - \langle D \rangle) \quad (8)$$

where $\langle \rangle$ denote averaged data and σ is the standard deviation. The SABER $\text{NO}^+(\text{v})$ VER data used in this analysis corresponds to six days during the Halloween 2003 storm event, from October 27 to November 1. The VER data were sorted and averaged into 5 degree magnetic latitude bins. In addition, the SABER $\text{NO}^+(\text{v})$ VER data and magnetic indices were sorted and averaged into 3-hour UT time bins throughout the six-day period. Figure 3 shows results from cross-correlations between SABER $\text{NO}^+(\text{v})$ VER data and four magnetic indices: HP (upper panel), ap, AE, and the absolute value of Dst (bottom panel). Each column represents a different altitude: 100 km, 110 km, 120 km, and 140 km, respectively. The vertical axes represent the Northern Hemisphere (NH) magnetic latitude and the horizontal axis is the delay time (τ in (8)) in hours. The colored contours correspond to the cross-correlation.

Since the HP index is a proxy for the physical source for the E-region response, HP will be considered the benchmark index to which the other magnetic indices will be compared. The broad features of the cross-correlations for each magnetic index separate into two distinct patterns. At 110 km and below, the peak cross-correlations are concentrated between 50 and 60 degrees in magnetic latitude, corresponding to the auroral oval region, and have an approximate zero response time. This feature is consistent with auroral dosing followed by fast ion-neutral reactions and prompted 4.3 μm emissions (Mertens et al., 2007a; Mertens et al., 2007b; Mertens et al., 2008). Above 110 km the peak cross-correlations extend to lower latitudes with a longer response time. It's possible for molecular rich air to be transported to midlatitudes from the auroral dosing region within six hours (Richards, 2004). Enhanced molecular rich air would produce enhanced NO concentrations by reactions of molecular oxygen with atomic nitrogen. Thus, the peak in the cross-correlation functions at low latitudes above 110 km could be due to horizontal transport of molecular oxygen. The direct transport of NO from the auroral dosing region to midlatitudes is still an open question (Richards, 2004). Further studies are required to understand Fig. 3 in detail. The main conclusion is that the common magnetic indices (ap, AE, and Dst) are comparable to our benchmark HP index in capturing the correlation between SABER $\text{NO}^+(\text{v})$ VER and auroral particle precipitation.

Since the ap index is already an input into IRI, ap may be the most practical index for use in IRI. Once the magnetic index is chosen, the parametric relation between SABER $\text{NO}^+(\text{v})$ VER SQR and the magnetic index can be implemented in the correction procedure described in Section 2. Since this procedure is based on the fundamental relations in (1)-(2), it is necessary to validate these relations. In the next section, SABER-ISR coincidences are found and the SQRs are compared.

4. SABER-ISR Coincidences

In order to validate (1)-(2), SABER and ISR coincident measurements are selected during different magnetic storms. Quiet periods are defined by $k_p < 3$. Magnetic active periods are defined by $k_p > 4$. Nighttime data is defined such that the solar zenith angle is greater than 104 degrees, which ensures no solar illumination below 200 km.

ISR measurements were selected from three different locations: EISCAT VHF at Tromso, Norway (69.59N, 19.23E), Loneyarbyen, Norway (78.15N, 16.03E), and Sondrestrom, Greenland (66.99N, 309.05E). Coincidences with SABER at each location were taken during three magnetic storm time events. To define a SABER/ISR spatial coincidence, the ISR location is centered in a magnetic latitude and longitude box that is extended ± 2.5 degrees in magnetic latitude and ± 10 degrees in magnetic longitude from the ISR location. To define a SABER/ISR time coincidence, we selected a 0.1 hour time difference between the SABER and ISR measurements. Each SABER measurement that fell within the magnetic box centered on the ISR locations, and fell within the selected time difference, was taken as a coincidence. ISR quiet time was taken within days prior to and following each magnetic storm, according to the availability of the data. On the other hand, SABER quiet times were selected according to the yaw maneuvers as depicted in Fig. 1. For example, if a SABER/ISR coincidence occurred in October, SABER quiet data from the yaw period corresponding to September 19 through November 21 are averaged for all years from 2002 until 2006. Figure 4 shows two SABER and EISCAT Tromso coincidences on October 30 (left panel) and October 31 (right panel), 2003. SABER and ISR SQR values show good agreement, especially from 114 km through 120 km. These two events occurred during the Halloween 2003 solar-geomagnetic storm events. ISR quiet data were taken from 10/06/2003-10/28/2003. The spatial-temporal differences between the SABER/ISR measurements are less for the event in the right panel compared to the left, corresponding to better agreement for the event in the right panel.

Figure 5 shows two SABER and Loneyarbyen ISR coincidences for October 29, 2003. These two scans are at the onset of the Halloween storm with k_p and Dst indices lower than the previous scans shown in Fig. 4. The ISR position is located further north, at the boundary of the auroral oval. In this case, the ISR experiment was performed with off-vertical beam measurements. ISR quiet data were taken from before (10/06/2003-10/25/2003) and after (11/02/2003-11/04/2003) the magnetic storm event. SABER quiet data dates were the same as in the previous case but with a different magnetic grid location. As can be seen from Fig. 5, results show similar agreement with the events in Fig. 4.

Figure 6 shows the final case study for SABER and ISR comparisons. ISR measurements are from the Sondrestrom facility with off-vertical beam measurements. The data shown are from a November 9, 2004 magnetic storm. Quiet ISR data are taken from before (10/22/2004-10/29/2004) and after (11/04/2004-11/05/2004) the November 2004 storm event. Since this event corresponds to the same SABER yaw cycle as the previous events in Figs. 4-5, SABER quiet data are taken from the same climatological period, but with a different magnetic grid location. As clearly seen in Fig. 6, SABER/ISR SQR comparisons show remarkable agreement in both cases.

4. Conclusions

Results derived from SABER $\text{NO}^+(\nu)$ VER measurements suggest that this product can be used as an effective proxy to monitor the response of the nighttime E-region ionosphere

to geomagnetic storm activity. We have demonstrated that we can derive a storm-time E-region electron density correction factor that can be directly applied to IRI. This conclusion is supported by two main results from this study. One, SABER $\text{NO}^+(\nu)$ VER SQR comparisons with ISR SQR show remarkable agreement for weak to strong magnetic storm activity. The SABER $\text{NO}^+(\nu)$ VER SQR is the fundamental quantity that will be used to develop a storm-time correction to E-region electron densities. Secondly, the cross-correlation studies between SABER $\text{NO}^+(\nu)$ VER and the common geomagnetic activity indices show comparable results to the benchmark SABER $\text{NO}^+(\nu)$ VER and HP index correlations. Since the HP index is indicative of the physical source responsible for the storm-time enhancements to the E-region electron density, this result indicates that the common geomagnetic indices can be used to parameterize the electron density enhancements with a simple magnetic driver index. Moreover, since the ap index is already an input variable in the IRI, our E-region storm model approach can be readily implemented in IRI. Our next steps will be to develop the parametric fit between storm-time SABER $\text{NO}^+(\nu)$ VER SQR and the geomagnetic activity indices, and validate our empirical storm-time E-region electron density correction with ISR measurements.

5. Bibliography

- Bilitza, D., International Reference Ionosphere. *Radio Science* 36(2), 261-265, 2001.
- Fox, J. L., Sung, K. Y. Solar activity variations of the Venus thermosphere/ionosphere. *J. Geophys. Res.* 106 (A10), 21,305-21,335, 2001.
- Mertens, C. J., Mast, J. C., Winick, J. R., Russell, J. M., III, Mlynczak, M. G., Evans, D. S. Ionospheric E-region response to solar-geomagnetic storms observed by TIMED/SABER and application to IRI storm-model development. *Adv. Space Res.* 39, 715-728, 2007a.
- Mertens, C. J., Winick, J. R., Russell, J. M., III, Mlynczak, M. G., Evans, D. S., Bilitza, D., Xu, X. Empirical storm-time correction to the International Reference Ionosphere Model E-region electron density parameterizations using observations from TIMED/SABER, in *Proceedings of the SPIE, Annual Meeting, Florence, Italy, September 17-19, vol. 6745, 2007b.*
- Mertens, C. J., Fernandez, J. R., Xu, X., Evans, D. S., Mlynczak, M. G., Russell III, J. M. A new source of auroral infrared emission observed by TIMED/SABER, *Geophys. Res. Lett.* 35, L17106, doi:10.1029/2008GL034701, 2008.
- Press, W. H., Teukolsky, S. A., Vetterling, W. T., Flannery, B. P. *Numerical Recipes in FORTRAN: The Art of Scientific Computing*, Cambridge University Press, New York, 1992.
- Richards, P. G., On the increases in nitric oxide density at midlatitudes during ionospheric storms, *J. Geophys. Res.*, 109, A06304, doi:10.1029/2003JA010110, 2004.
- Russell, J. M., III, Mlynczak, M. G., Gordley, L. L., Tansok, J., Esplin, R. An overview of the SABER experiment and preliminary calibration results, in *Proceedings of the SPIE, 44th Annual Meeting, Denver, Colorado, July 18-23, vol. 3756, 277-288, 1999.*
- Torr, M. R., Torr, D. G., Richards, P. G., Yung, S. P. Mid- and low-latitude model of thermospheric emissions 1. $O^+(^2P)$ 7320 Å and $N_2(^2P)$ 3371 Å. *J. Geophys. Res.* 95 (A12), 21,147-21,168, 1990.
- Vassiliadis, D., Klimas, A. J., Kanekal, S. G., Baker, D. N., Weigel, R. S. Long-term average, solar cycle, and seasonal response of magnetospheric energetic electrons to the solar wind speed, *J. Geophys. Res.*, 107(A11), 1383, doi:10.1029/2001JA000506, 2002.

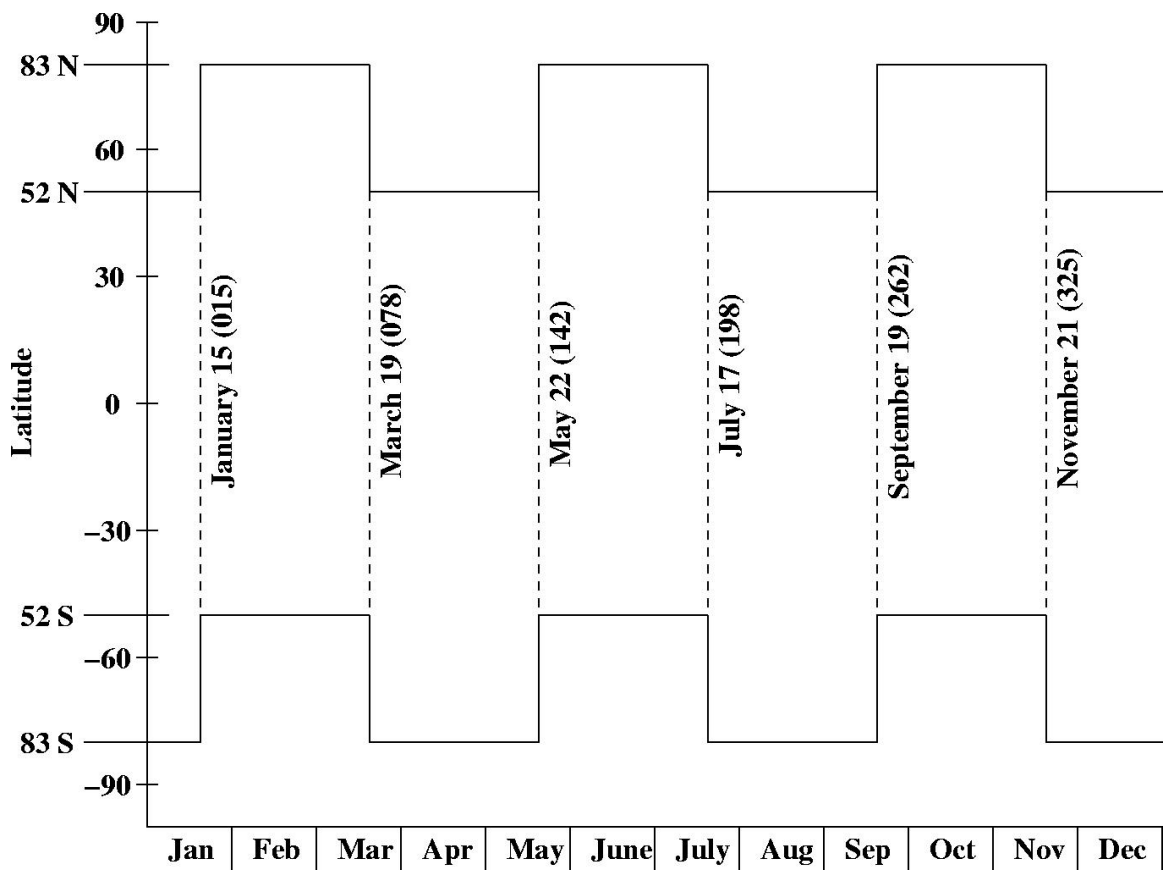


Figure 1: TIMED/SABER latitude coverage during 2003. Dashed line indicates the yaw maneuvers.

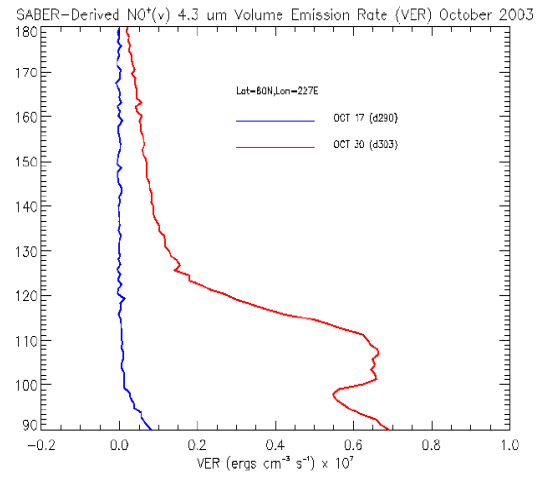
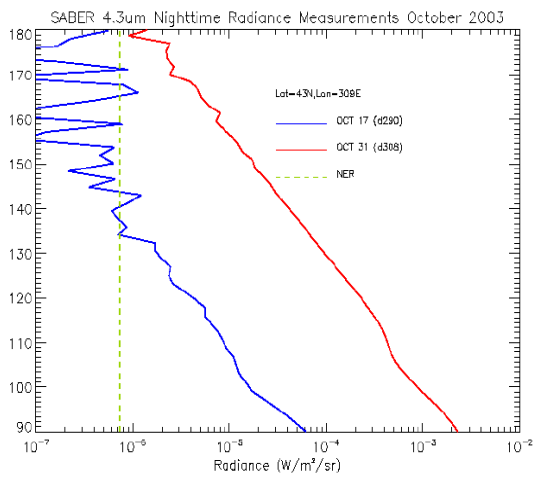


Figure 2: Nighttime radiance and VER measurements before (blue line) and during (red line) Halloween 2003 magnetic storm.

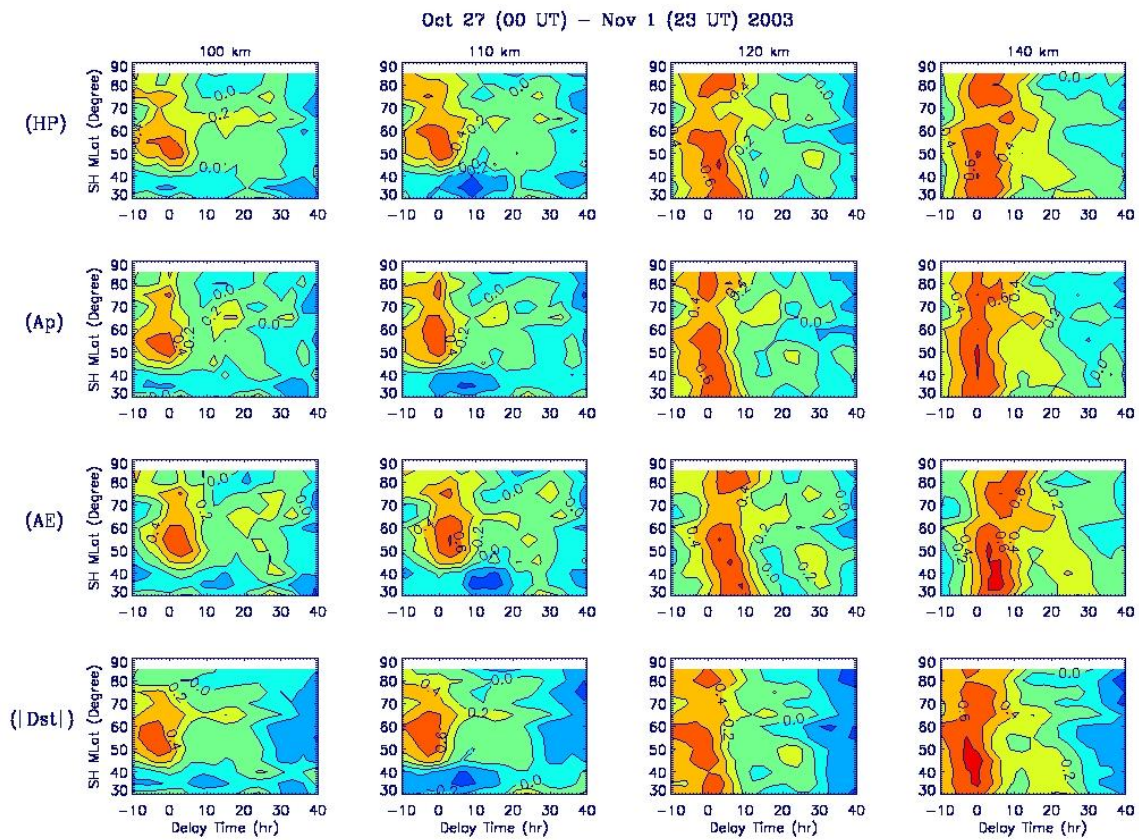


Figure 3: Cross correlation between $\text{NO}^+(\nu)$ VER and HP, ap, AE, and $|\text{Dst}|$ indices for October 27 (00 UT)-November 1 (23 UT), 2003.

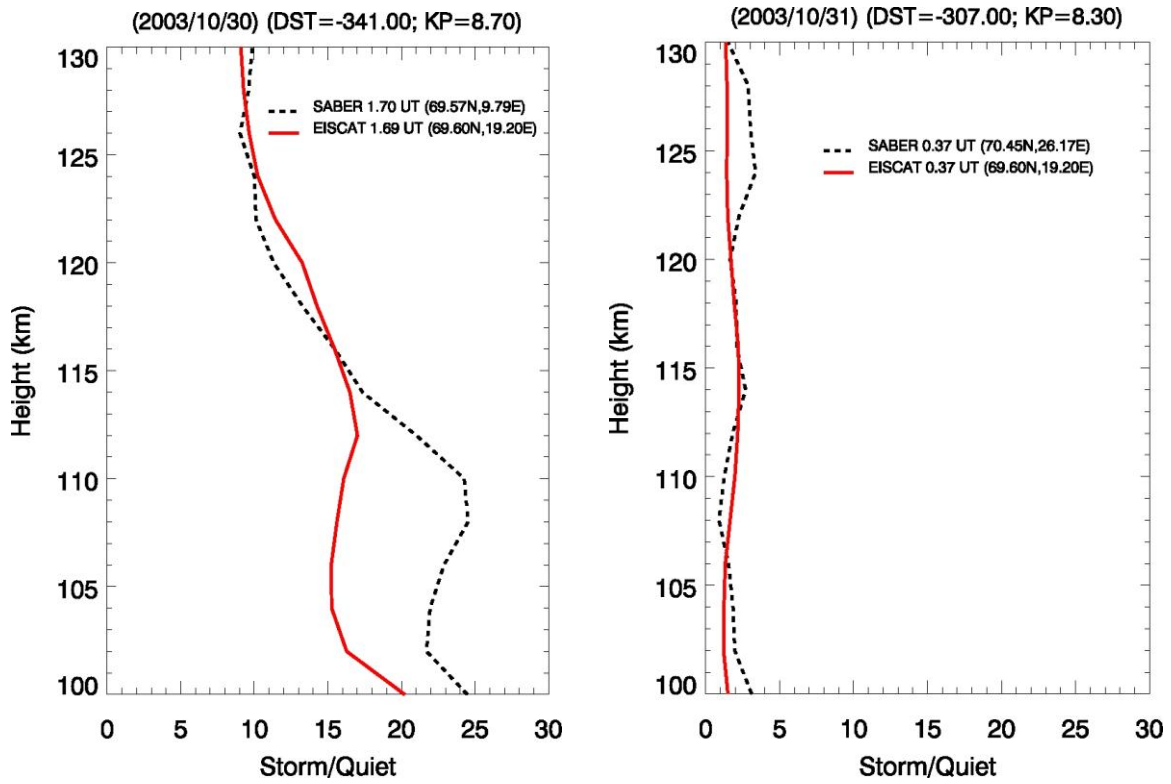


Figure 4: EISCAT VHF and SABER $\text{NO}^+(\nu)$ VER SQR comparisons for October 30 and October 31, 2003.

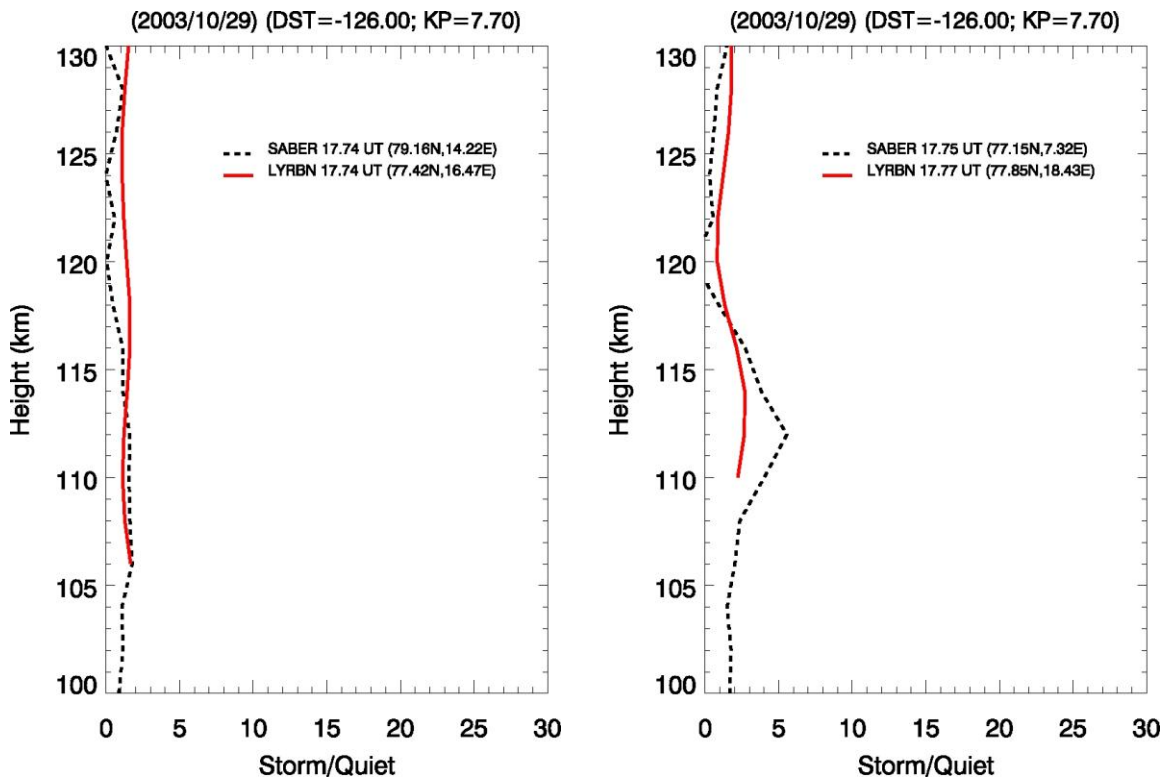


Figure 5: SABER and Loneyarbyen SQR comparisons for October 29, 2003. The Loneyarbean profile was constructed locations from off-vertical beam measurements.

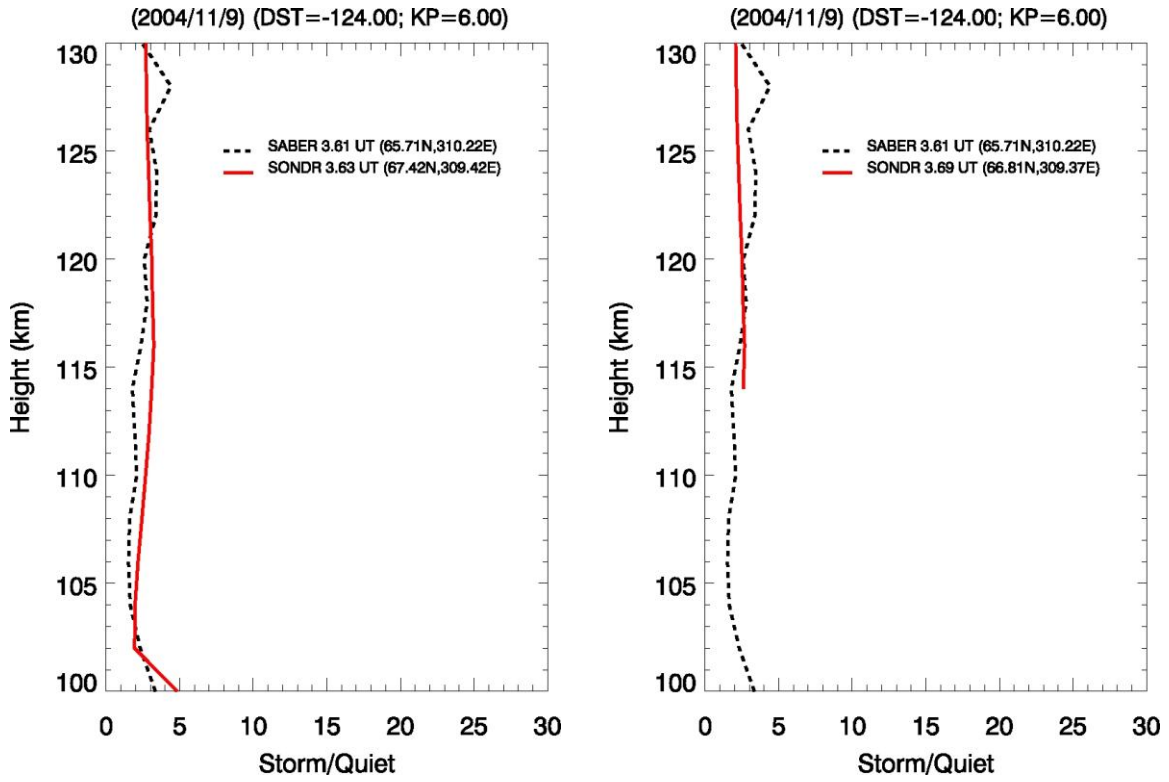


Figure 6: SABER and Sondrestrom SQR comparisons for November 09, 2004 magnetic storm.